BDNF controls neuropsychiatric manifestation via autophagic regulation of p62 and $GABA_A$ receptor trafficking

Toshifumi Tomoda,[1,2,*] Akiko Sumitomo,[1,2] Yuki Hirota-Tsuyada,[2] Hitoshi Miyachi,[3] Hyunjung Oh,[1] Leon French,[1] and Etienne Sibille,[1,*]

[1]Campbell Family Mental Health Research Institute, Centre for Addiction and Mental Health, University of Toronto, Toronto, Ontario M5T 1R8, Canada.
[2]Department of Research and Drug Discovery, Medical Innovation Center, Kyoto University Graduate School of Medicine, Kyoto 606-8507, Japan.
[3]Institute for Virus Research, Kyoto University, Kyoto 606-8507, Japan.

*Correspondences: ttomoda1@gmail.com
Etienne.sibille@camh.ca

Key words: BDNF, p62, α5$GABA_A$ receptor trafficking, autophagy

SUMMARY

Reduced expression levels of brain-derived neurotrophic factor (BDNF) and disturbances of γ-aminobutyric acid (GABA) neurotransmission have been reported in several neuropsychiatric conditions, incluing major depressive disorder (MDD). Although we previously showed a causal link between repressed BDNF signaling and deregulated GABA neurotrasnmission, a mechanistic link between these two pathways remained elusive. Here, we show that mice heterozygous for *Bdnf* have upregulated expression of sequestosome-1/p62, an autophagy-associated stress response protein, in the pyramidal neurons of the prefrontal cortex (PFC), and exhibit behavioral deficits relevant to the PFC dysfunctions, including cognitive inflexibility and sensorimotor gating deficits. *Bdnf* heterozygous (*Bdnf*$^{+/-}$) neurons showed reduced surface expression of α5 subunit of $GABA_A$ receptor (α5$GABA_A$R) in the PFC. Genetically reducing *p62* gene dosage restored the α5$GABA_A$R surface expression and rescued the behavioral deficits in *Bdnf* $^{+/-}$ mice. Moreover, gene profiling analysis suggested overall reduction in autophagic activity in the corticolimbic area of the MDD brains. Thus, the current study reveals a novel mechanism by which p62 dosage control (*i.e.*, autophagy regulation) serves as a converging point that links reduced BDNF signaling, GABA deficits, and impaired cognition.

INTRODUCTION

Cognitive impairment is a hallmark symptom associated with a range of psychiatric and neurological conditions (1, 2), manifesting either as a core symptom of major mental illnesses or age-related decline of brain functions, or as a condition comorbid to neurodegenerative and other brain disorders. Pathobiological mechanisms underlying cognitive impairment include deficits in neural plasticity or synaptic functions (3); however, diverse molecular entities and multiple neurotransmitter systems that support synaptic function and plasticity make it hard to understand central neurobiological events contributing to cognitive dysfunction, and to identify therapeutic leads that can effectively be targeted to alleviate this symptom.

Major depressive disorder (MDD) is the most frequent psychiatric condition characterized by several different symptomatologies, including low mood, anhedonia, physical disturbance, and cognitive dysfunction (4). MDD affect ~5.3% of the population worldwide in a given year, with a lifetime prevalence of ~13.2%, presenting major burdens at personal and socioeconomic levels (5). Conventional antidepressant medications, most of which act via the monoaminergic system (*e.g.*, selective serotonin reuptake inhibitors [SSRIs]) (6, 7), are only effective in alleviating some of the symptoms in a subset of patients, presenting limited remission rates

(~30%) or ultimate ineffectiveness after long-term use. Although rapid-acting antidepressants have shown promise in preclinical studies and effectiveness in treating severely depressed individuals (8), no existing antidepressant drug directly targets the pathophysiology observed in the depressed brain, providing a potential explanation for the limited efficacy of current antidepressants.

Previous translational and molecular studies have consistently demonstrated lower expression levels of brain-derived neurotrophic factor (BDNF) in the postmortem brains of MDD patients and of rodent models (9, 10). Reduced levels of BDNF have also been reported for additional psychiatric conditions, including schizophrenia (11–13) and age-related cognitive decline (14, 15). Animal models with reduced BDNF expression or activity showed disturbances of neurotransmission or neural plasticity, which likely underlie cognitive deficits observed in these models (16–18), suggesting a critical role of this pathway in the deterioration of cognitive dimension shared across a range of psychiatric conditions.

BDNF is a member of the neurotrophin family of growth factors (19) and plays a number of critical roles in the nervous system, including neuronal survival, proliferation, synaptogenesis, neurotransmission, learning, memory, and cognition (16, 20). BDNF primarily

signals through binding to TrkB receptor and its co-receptor, p75/NTR, leading to activation or modulation of downstream signaling molecules (19). BDNF signaling could also be regulated at the receptor level; upon ubiquitination of TrkB and p75/NTR by an E3 ligase TRAF6, the ubiquitin-binding adaptor protein, sequestosome-1/p62, is recruited to form a protein complex (TrkB/TRAF6/Ubi/p62), which is then trafficked to an appropriate cellular compartment (*e.g.*, the proteasome or lysosome for degradation, the endosome for internalization or recycling), leading to down- or up-regulation of BDNF signaling in a context-dependent manner (21). p62 is an adaptor protein that could integrate multiple cellular processes, including growth factor signaling, ubiquitin/proteasomal system, and autophagy/lysosomal system, by interacting with signaling molecules, ubiquitinated proteins, and autophagy-related protein LC3, respectively (22). However, despite cumulative knowledge on BDNF signaling, it remains elusive how BDNF modulates circuit-wide mechanisms to regulate higher-order brain functions, such as cognition.

Besides BDNF, we and others have consistently demonstrated dysfunctions of γ-aminobutyric acid (GABA)-mediated neurotransmission in the corticolimbic circuitry of MDD patients and of rodent models (10, 23–25).

Deregulated GABAergic neurotransmission has also been reported for schizophrenia (26, 27) and age-related cognitive decline (28), suggesting central importance of this inhibitory pathway in the pathophysiology of mental illnesses. To address a possible link between reduced BDNF levels and deregulated GABA neurotransmission, we have recently taken an unbiased gene expression profiling approach to identify genes whose expressions were positively correlated with BDNF and analyzed them for enriched biological pathways, using orbitofrontal cortex samples from young vs. old human subjects (14). We confirmed age-related downregulation of BDNF and showed 78 of the top 200 BDNF-coexpressed genes were associated with synaptic function, including those expressed in GABA synapses. Overall, ~68.4% of GABA synaptic genes showed decreased expression with age and the majority were positively correlated with BDNF expression levels. In addition, blockage of BDNF signaling in mice led to reduction in expression of these GABA synaptic genes, demonstrating a causal link between repressed BDNF signaling and deregulated GABA-mediated inhibitory neurotransmission (14). Of particular interest was the α5 subunit of $GABA_A$ receptor ($\alpha5GABA_AR$), whose expression was significantly decreased in aged human brains and in mice with repressed BDNF signaling (14). Because $\alpha5GABA_AR$ is predominantly expressed by

pyramidal neurons in corticolimbic area of the brain and shown to be responsible for cognitive function (29), we hypothesized that correlative dysregulation of BDNF and α5GABA$_A$R expression may underlie cognitive deficits observed across neuropsychiatric conditions.

In the present study, we first addressed a new mechanism by which BDNF controls cell surface presentation of α5GABA$_A$R, via regulation of p62 expression levels. We then used *Bdnf* heterozygous (*Bdnf*$^{+/-}$) mice to address a functional link between attenuated BDNF signaling and reduced α5GABA$_A$R surface expression, by evaluating deficits in cognitive flexibility and sensorimotor gating, which are endophenotypes relevant to psychiatric manifestation (30, 31). Finally, we analyzed the relevance of the pathway regulating p62 levels (*i.e.*, autophagy) to neuropsychiatric manifestation, using the gene expression dataset from MDD cohorts. We predicted that controling p62 levels may serve as a converging point that links reduced BDNF signaling, GABA deficits, and impaired cognition.

RESULTS

BDNF regulates autophagy in cortical neurons

A recent study reported evidence that TrkB is located to the autophagosome and mediates retrograde transport of this organelle in neurons (32), suggesting a potential role of BDNF signaling in autophagy. Autophagy is a specialized membrane trafficking machinery and a major cellular recycling system responsible for degrading old proteins and damaged organelles in the lysosome, which ultimately serve as resources to generate new proteins and energy, and thus critical to the maintenance of cellular homeostasis (33).

As a first step to address the role of BDNF in neuronal autophagy, we prepared primary cortical neurons from transgenic mice expressing GFP-LC3, a fluorescent marker for the autophagosome (34), and cultured them for 16 days before treating them with BDNF (100 ng/ml) for 30 min. We observed an increase in number and size of GFP-LC3-positive punctate structures (**Fig. 1A**), suggesting either *de novo* autophagosome formation due to autophagy induction or the accumulation of LC3 due to attenuated autophagic degradation. To discriminate between these two possibilities, we performed the autophagy flux assay (35); BDNF increased the autophagy flux (*i.e.*, the difference between the amount of membrane-bound LC3 (*i.e.*,

LC3-II) seen in the presence vs. the absence of lysosomal protease inhibitors, which reflects the amount of LC3 degraded through an autophagy-dependent process within the lysosome) (**Fig. 1B**), suggesting that BDNF has an autophagy-inducing activity. We next tested whether BDNF could affect the later phase of autophagy (*i.e.*, maturation stage), which can be assessed by evaluating the acidicity of the autophagosome/lysosomal system using LysoTracker (35). To facilitate simultaneous observation of autophagosome formation and maturation, primary cortical neurons prepared from wild-type (WT) mice were transfected with GFP-LC3 and then labeled with LysoTracker for the last 5 min of the culture period 30 min after adding BDNF in culture. BDNF markedly increased the extent of LysoTracker uptake by the soma (**Fig. 1C**), indicating that BDNF enhanced maturation of the autophagy/lysosomal system in neurons. Consistently, neurons with greater levels of LysoTracker uptake exhibited increase in number and size of the autophagosome located to the neurite (**Fig. 1C**, arrows).

Reduced BDNF expression leads to elevated p62 levels in cortical pyramidal neurons

To address the intrinsic activity of BDNF in the regulation of autophagy *in vivo*, we quantitated the level of p62 protein in the medial prefrontal cortex (mPFC) of *Bdnf*$^{+/-}$ mice. In this region of

the brain, BDNF is predominantly produced by CaMKII-positive pyramidal neurons and functions as an autocrine and paracrine factor to modulate the activity of neighboring excitatory and inhibitory neurons (9). p62 has been used as an *in vivo* marker of autophagic activity, because this protein serves as a selective target for autophagic degradation (35). We found significantly increased levels of p62 protein in CaMKII-positive neurons in *Bdnf*$^{+/-}$ mice, as compared with WT control mice (**Fig. 2A, B**). This increase is not likely due to transcriptional upregulation of *p62* gene expression (**Fig. 2C**), implying that the increased levels of p62 may result from reduced rates of protein degradation, consistent with the idea that BDNF serves as an intrinsic factor that enhances autophagy. To further obtain evidence to support this idea, we quantitated levels of expression of additional autophagy-related genes in the mPFC of *Bdnf*$^{+/-}$ mice. Expression of several autophagy regulatory genes (*e.g.*, *Lc3*, *Gabarap*, *Ulk2*) remained unchanged, whereas expression of *Ulk1*, a gene critical to autophagy induction (33), was significantly downregulated by ~25% (**Fig. 2C**), providing a potential mechanism underlying attenuated autophagy in *Bdnf*$^{+/-}$ mice.

Elevated p62 expression in *Bdnf*$^{+/-}$ cortical neurons causes downregulated surface

presentation of α5GABA$_A$R

Although the data showed that decreased expression of BDNF resulted in elevated levels of p62 protein in part through attenuated autophagy in neurons, questions remain as to how repressed BDNF signaling can be linked to deregulated GABA neurotransmission. In particular, α5GABA$_A$R was among the genes most significantly correlated with BDNF, as depicted by our previous study (14), and both of these genes are predominantly expressed by the pyramidal neurons in the mPFC (9, 14). Because p62 is reported to interact with GABA$_A$ receptor-associated protein (GABARAP) (36), which regulates endocytic trafficking of GABA$_A$ receptors in neurons (37), we reasoned that the elevated p62 expression in *Bdnf*$^{+/-}$ neurons may influence surface presentation of α5GABA$_A$R.

Surface biotinylation of cultured cortical neurons showed that levels of cell surface α5GABA$_A$R expression were reduced in *Bdnf*$^{+/-}$ neurons, as compared with WT control neurons. Reducing the *p62* gene dosage in *Bdnf*$^{+/-}$ neurons (*Bdnf*$^{+/-}$;*p62*$^{+/-}$) restored the surface α5GABA$_A$R to levels comparable to those in WT (**Fig. 3A**). In addition, receptor cross-linking assays using bis(sulfosuccinimidyl)suberate (BS3) (38), a membrane-impermeable chemical cross-linker, confirmed that the surface levels of α5GABA$_A$R expression were significantly

reduced in the prefrontal cortex of *Bdnf*$^{+/-}$ mice, whereas those in *Bdnf*$^{+/-}$;*p62*$^{+/-}$ mice were equivalent to those in WT (**Fig. 3B**). Thus, decreased BDNF expression results in reduced surface presentation of α5GABA$_A$R through elevated p62 expression in the PFC.

Elevated p62 expression in *Bdnf*$^{+/-}$ mice causes behavioral deficits relevant to the PFC dysfunction

We then questioned whether and how the elevated p62 expression in *Bdnf*$^{+/-}$ mice affects the PFC-relevant brain functions, such as information processing and cognition. Previous studies reported that *Bdnf*$^{+/-}$ mice had reduced prepulse inhibition (PPI) of acoustic startle response (39), demonstrating a role of BDNF in sensorimotor gating function. This mechanism of filtering sensory information to render appropriate motor responses has been shown to rely in part on the function of the cortical circuitry involving mPFC (40). In agreement with the previous study, we showed that *Bdnf*$^{+/-}$ mice had reduced levels of PPI (**Fig. 3C**). Reducing the *p62* gene dosage in *Bdnf*$^{+/-}$ mice (*i.e.*, *Bdnf*$^{+/-}$;*p62*$^{+/-}$) rescued the PPI to levels equivalent to those in controls (**Fig. 3C**). The data suggest that decreased expression of BDNF results in sensorimotor gating deficits through elevated p62 expression in the nervous system.

A recent study reported impaired cognitive flexibility in *Bdnf*$^{+/-}$ mice, using visual discrimination cues to evaluate cognitive functions (41). To further address deficits in cognitive flexibility in *Bdnf*$^{+/-}$ mice, we used a rule shifting paradigm (42, 43), in which mice were initially trained to associate food reward with a specific stimulus (*i.e.*, either an odor or a digging medium) and subsequently evaluated for cognitive flexibility by changing the type of stimulus that predicts the reward (**Fig. 3D**). Although both *Bdnf*$^{+/-}$ and WT mice learned the association rule in a similar number of trials during the initial association phase of trials, *Bdnf*$^{+/-}$ mice were specifically impaired during the rule shifting phase of trials (**Fig. 3E**). When the *p62* gene dosage was reduced in *Bdnf*$^{+/-}$ mice (*i.e.*, *Bdnf*$^{+/-}$;*p62*$^{+/-}$), the mice showed cognitive performance indistinguishable from that of controls (**Fig. 3E**). The data suggest that decreased expression of BDNF results in cognitive deficits through elevated p62 expression in the nervous system.

Elevated p62 expression is sufficient to cause downregulation of surface α5GABA$_A$R expression and behavioral deficits

To further address the causal role of elevated p62 expression in the regulation of α5GABA$_A$R surface expression and the associated behavioral changes, we generated p62-Tg mice, in which

p62 transgene expresion was driven by CaMKII promotor. Among three transgenic lines established, 2 lines (#1, #2) showed ~60% increase in the level of p62 protein expression in the PFC, while the third line (#3) failed to overexpress p62 as evaluated by Western blot (**Fig. 4A**). BS3 cross-linking assays demonstrated that the PFC of the p62 overexpressing line (#1) had reduced levels of surface $\alpha5GABA_AR$ expression compared to WT, whereas non-overexpressing line #3 had surface $\alpha5GABA_AR$ expression equivalent to the WT (**Fig. 4B**).

When the semsorimotor gating was evaluated for these p62-Tg lines, p62 overexpressing lines (#1, #2) exhibited reduced levels of PPI, whereas the non-overexpressing line #3 had equivalent levels of PPI compared to the WT (**Fig. 4C**). We then assesed the congnitive flexibility of p62-Tg mice (line #1) as compared with WT. Although p62-Tg mice learned the association rule during the initial association phase of trials in a similar manner to WT, p62-Tg mice were impaired during the rule shifting phase of trials (**Fig. 4D**). These data confirmed the causal role of elevated p62 expression in the PFC-relevant behavioral deficits.

Gene expression profiling suggests altered autophagy machinery in MDD brains

Although reduced levels of expression and/or functioning of BDNF and $\alpha5GABA_AR$ are

consistently reported in the brains of several neuropsychiatric conditions (9–15, 23–28), including MDD, the cellular machinery that may underlie these changes remains to be understood. Given our present data demonstrating elevated p62 levels in *Bdnf*$^{+/-}$ mouse model, we hypothesized that alteration in the autophagy machinery may in part account for cellular deficits present in the affected brains.

To test this hypothesis, we analyzed the gene expression profiles in the corticolimbic area of the MDD brain cohorts that were previously compiled from 8 independent microarray datasets collected from ~51 patients and ~50 controls (44). Autophagy-related genes we tested were primarily those defined by the gene ontology (GO) term (45, 46). Among the 77 genes included in the GO term "positive regulation of autophagy" (GO.0010508), 1 gene showed a significant increase ($P < 0.05$) compared to the control cohorts and 29 genes showed an increasing trend with no statistical significance, whereas 6 genes showed a significant decrease ($P < 0.05$) and 41 genes showed a decreasing trend with no statistical significance (**Supplementary Table 1**). In addition, among the 28 genes included in the GO term "autophagosome maturation" (GO.0097352), 11 genes showed an increasing trend with no statistical significance, whereas 2 genes showed a significant decrease ($P < 0.05$) and 15 genes

showed a decreasing trend with no statistical significance (**Supplementary Table 2**). By contrast, among the 38 genes included in the GO term "negative regulation of autophagy" (GO.0010507), 3 genes showed a significant increase compared to the control cohorts and 22 genes showed an increasing trend with no statistical significance, whereas 2 genes showed a significant decrease and 11 genes showed a decreasing trend with no statistical significance (**Supplementary Table 3**). To characterize the overall trend for gene expression of autophagy-related genes, we generated a custom list of "autophagy-enhancing genes" by compiling the GO term "positive regulation of autophagy" and the GO term "autophagy maturation", as well as another custom list of "autophagy-attenuating genes" by removing, from the GO term "negative regulation of autophagy", 4 genes that were also categorized in the GO term list "positive regulation of autophagy". When the levels of expression of the autophagy-enhancing genes vs. the autophagy-attenuating genes were compared, a significant difference was observed between these two groups (P = 0.0077) (**Fig. 5A**), with the former tended to cluster toward the direction of downregulation, whereas the latter tended to cluster toward the direction of upregulation (**Fig. 5B**). As internal reference, levels of gene expression of *BDNF* and *Somatostatin* (*SST*) were plotted, both of which have been reported to be

significantly downregulated in the corticolimbic area of the MDD brains (44).

DISCUSSION

Our previous study showed that reduced BDNF expression in the mPFC causes selective attenuation of GABAergic inhibitory neurotransmission through transcriptional control of GABA-related genes (14). In the present study, we demonstrated an additional layer of mechanism by which reduced BDNF signaling negatively impacts GABA functions via control of $GABA_A$ receptor trafficking. Importantly, our data suggest for the first time that dosage control of p62 provides a key molecular event that links BDNF signaling, GABAergic neurotransmission, and cognitive and other behavioral outcomes relevant to the PFC functions.

Neuropsychiatric diseases have been shown to occur through a complex interaction of multiple genetic and environmental risk factors; the latter includes chronic psychosocial stress in the case of MDD (25), and BDNF was identified as a protein downregulated in response to such psychosocial stresses (9, 10). In addition, we have provided compelling evidence that, in response to reduced BDNF activity in the pyramidal neurons of the mPFC, expression levels of presynaptic genes (*e.g.*, *Gad1*, *SLC32A1*) and neuropeptide genes (*e.g.*, *SST*, *neuropeptide Y*,

cortistatin) expressed in the neighboring inhibitory neurons were significantly downregulated (14), suggesting a paracrine mode of BDNF action responsible for attenuated GABA signaling (**Fig. 6**, right). Moreover, expression levels of *Gabra5*, a gene encoding α5$GABA_A$R that is predominantly targeted to the dendritic compartment of the pyramidal neurons, were among the most significantly downregulated, suggesting an autocrine mode of BDNF action contributing to reduced expression of GABA-related genes. Both modes of transcriptional mechanisms, coupled with attenuated $GABA_A$ receptor trafficking demonstrated in the current study (**Fig. 6**, left), are expected to amplify pathophysiological consequences leading to deregulated GABA neurotransmission.

p62 was originally identified as a protein induced by cellular stress condition (22, 33), and subsequently shown to function as an adaptor protein that could integrate multiple cellular processes, including the autophagy/lysosomal pathway (22). Autophagy is activated in response to a range of cellular stresses (*e.g.*, depletion of nutrients and energy, misfolded protein accumulation, oxidative stress) and mitigates such stresses to maintain cellular homeostasis (33). Thus, this pathway has a potential to serve as a cellular machinery to combat cellular stresses elicited by psychosocial insults. The gene expression profiling data suggested that

overall activity of autophagy machinery may be attenuated in the brains of MDD, which likely compromises functional homeostasis of circuitry mechanisms, through elevated p62 expression and hence downmodulated $GABA_A$ receptor trafficking.

Cognitive function is primarily controlled via the corticolimbic circuitry mechanisms, in part through regulation of excitatory and inhibitory neurotransmission (27, 30). A number of synaptic genes have been implicated in this process, including BDNF and $\alpha5GABA_AR$. *Bdnf*$^{+/-}$ mice are reported to exhibit reduced amplitude and frequency of miniature currents (mIPSC) in cortcial and thalamic neurons (47), which possibly underlies cortical circuitry disturbances leading to cognitive inflexibility or sensorimotor gating deficits observed in these mice. Likewise, mice deficient for $\alpha5GABA_AR$ also exhibit cognitive inflexibility (29) and sensorimotor gating deficits (48). Given the critical role of p62 in the regulation of these behavioural outcomes and $\alpha5GABA_AR$ trafficking in *Bdnf*$^{+/-}$ mice, as demonstrated in the present study, we propose that these molecular players (*i.e.*, p62, BDNF, $\alpha5GABA_AR$) have central importance in the regulation of cognitive dimension and other brain function. Notably, levels of p62 protein accumulation are expected to increase with age, as a reflection of gradual decrease in cellular autophagy activity (49). Moreover, elevated levels of p62 or increase in p62$^+$

inclusions are the cardinal feature commonly observed in neurodegenerative disorders, including Alzheimer's disease and Parkinson's disease (50, 51). Controlling the dosage of p62 protein may provide a potential target for therapeutic intervention against symptoms shared among these disorders, such as cognitive impairment, through augmentation of inhibitory neurotransmission. In particular, surface availability of $GABA_A$ receptors represents a rate-limiting step for GABAergic neurotransmission. Therefore, the mechanisms for regulating surface presentation of $GABA_A$ receptor through p62 dosage control may provide an alternative therapeutic approach for those who do not respond to current treatment of MDD or other neuropsychiatric disorders.

MATERIALS AND METHODS

Animals

Bdnf knockout mice (*Bdnf* ^{tm1Jae}/J, stock No. 002266) were obtained from The Jackson Laboratory (Bar Harbor, USA). GFP-LC3 transgenic mice were provided by Dr. Noboru Mizushima (University of Tokyo, Japan). p62 knockout mice were provided by Dr. Toru Yanagawa (University of Tsukuba, Japan). CaMKII-p62 transgenic mice were generated according to the standard procedures (52). Mice were maintained on the C57BL/6J genetic background for at least 10 generations. Eight to 12-week old male mice were used for behavioral analysis. Behavioral experiments and data collection were performed by the experimenters who were blinded to animal genotypes. Maintenance of mouse colonies and experiments using mice were in accordance with the NIH Guide for the Care and Use of Laboratory Animals, and approved by the Institutional Animal Care and Use Committee at Kyoto University and at the Centre for Addiction and Mental Health affiliated with University of Toronto.

Prepulse inhibition

The startle response and prepulse inhibition (PPI) were measured using a startle reflex measurement system (SR-LAB) as described (53), with minor modifications. The test session began by placing a male mouse in a plastic cylinder and leaving it undisturbed for 30 min. The background white noise level in the chamber was 70 dB. A prepulse−pulse trial started with a 50-ms null period, followed by a 20-ms prepulse white noise (74, 78, 82, 86, or 90 dB). After a 100-ms delay, the startle stimulus (a 40-ms, 120 dB white noise) was presented, followed by a 290-ms recording time. The total duration of each trial was 500 ms. A test session consisted of six trial types (pulse-only trial, and five types of prepulse−pulse trial). Six blocks of the six trial types were presented in a pseudorandomized order such that each trial type was presented once within a block. The formula 100−((Response on acoustic prepulse−pulse stimulus trials/Startle response on pulse-only trials) x 100) was used to calculate %PPI.

Rule shift assay

Cognitive flexibility was evaluated in the rule-shifting assay, essentially as described (42, 43). In brief, mice were habituated to food, feeding apparatus, different odor cues and digging

medium texture cues prior to testing, and then food-deprived a day before the assays. Mice were initially trained in a sequence of trials to associate a food reward with a specific stimulus (*i.e.*, either an odor or a digging medium). A varying combination of stimulus and food reward was presented to mice per trial. Eight consecutive correct responses to the food reward were considered reaching criterion (*i.e.*, successful establishment of association between the stimulus and the food reward), and the number of trials to reach criterion were scored for each mouse tested before and after rule shifting (*e.g.*, from an odor cue to a different texture cue to predict reward). Upon rule shifting, numbers of errors due to perseveration to an old rule were scored before reaching new criterion.

Quantitative reverse transcription-polymerase chain reaction (qRT-PCR)

Total RNA was extracted from the ACC using RNeasy Mini kit (Qiagen), and reverse-transcribed with a ReverTra Ace cDNA synthesis kit (Toyobo). TaqMan probes were purchased from Applied Biosystems, Inc. All data were normalized with *Gapdh* as reference.

Primary cortical neuron culture

Primary cortical neurons were prepared from E13.5 frontal cortex through papain treatment (0.5 μg/ml in Earle's balanced salt solution supplemented with 5 mM EDTA and 200 μM L-cysteine), followed by mechanical trituration using fire-bore glass pipettes, and plated on poly-D-lysine-coated glass cover slips or glass-bottom dishes (MatTek). The cultures were recovered in serum-containing media (Neurobasal media supplemented with 10% horse serum, 5% fetal bovine serum, and 2 mM glutamine [Gibco]) for 4 h and maintained in serum-free media (Neurobasal media supplemented with B-27 (1:50 diluted), 2 mM glutamine, 50 I.U./ml penicillin, and 50 μg/ml streptomycin), with half of media being replaced with fresh media every 2−3 days. The cultures were used for immunofluorescence analysis or for surface biotinylation followed by Western blot analysis.

Immunofluorescence analysis

Primary cortical neurons cultured for 18–25 days were transfected with GFP-LC3 expression plasmid using Lipofectamine 2000 (Invitrogen) via the standard procedure, and 48 h post-transfection, the cells were incubated with BDNF (Sigma, 100 ng/ml) for up to 40 min

before fixation with 4% paraformaldehyde (PFA) in PBS. When appropriate, LysoTracker (Invitrogen) was included in culture media for the last 5 min of culture period before fixation. Fluorescence images were acquired by confocal microscopy (SP8, Leica) and the fluorescence intensities of GFP+ puncta and LysoTracker uptake were evaluated by ImageJ (NIH).

Surface biotinylation

Biotinylation of cell surface proteins was performed in primary neuron cultures using the cell surface protein isolation kit (Pierce) according to the manufacturer's protocol. Briefly, cells were incubated with ice-cold PBS containing Sulfo-NHS-SS-Biotin (Pierce) for 30 min with gentle rocking at 4°C. Cells were then lysed and precipitated with NeutrAvidin beads. Precipitated proteins were eluted from the NeutrAvidin beads with loading buffer containing dithiothreitol and heated for 5 min at 95°C and then analyzed by Western blot.

Chemical cross-linking assay

Cell surface receptor cross-linking assays were performed as described (38). In brief, mice were decapitated and the coronal brain slices (~1 mm thick) were quickly prepared using Brain

Matrix (Ted Pella) within 30 sec on ice. The prefrontal cortex was then excised from the slices, minced into pieces using a razor blade, and incubated in artificial CSF buffer containing bis(sulfosuccinimidyl)suberate (BS3) cross-linker (2 mM, ThermoFisher) for 30 min to 4 h at 4°C with constant invert mixing. After quenching the crosslinking reaction by adding glycine (100 mM) for 10 min at 4°C, the tissues were harvested by centrifugation (20,000 *g*, 4°C, 2 min). The proteins were prepared in lysis buffer containing 0.1 % Nonidet P-40 (v/v), protease inhibitor and phosphatase inhibitor cocktail, and 1 mM dithiothreitol, and analyzed by Western blot.

Western blots

Western blot analysis was performed according to the standard procedure. The primary antibodies used were anti-$GABA_A$ receptor α5 subunit (rabbit, 1:1,000, R&D Systems), anti-NR1 (rabbit monoclonal [1.17.2.6], 1:1,000, Millipore), anti-p62 (guinea pig, 1:1,000, MBL), anti-LC3B (rabbit, 1:1,000, Novus), anti-GAPDH (mouse, 1:1,000, abcam), and anti-α-Tubulin (mouse monoclonal [B-5-1-2], 1:8,000, Sigma).

Immunohistochemistry

For immunohistochemical analysis, brains of perfused mice (n = 4 per group) were serially cut into 50 μm-thick coronal sections using vibratome (VT1200S, Leica), and the sections from one cohort of mice (a littermate pair of wild-type and *Bdnf*$^{+/-}$ mice) were permeabilized in PBS containing 0.05% Triton X-100 for 1 h, and incubated for 30 min at room temperature in 10% goat serum (Chemicon) in PBS, and simultaneously immunostained for 16 hours at 4°C with primary antibodies followed by Alexa Fluor® 488- or 546-conjugated secondary antibodies (Molecular Probes) for 1 h at room temperature. The stained samples were observed using a confocal microscope (SP8, Leica; 40x objective lens, NA = 1.3); images of one optical section (1 μm thick) were acquired from 3 to 6 non-overlapping areas per section, randomly chosen in each brain region (prefrontal cortex), and 3 to 4 serial sections were analyzed. The fluorescence intensities of p62 immunostaining were measured from each neuronal soma (30~50 somas per section) using ImageJ (NIH), with the background levels of staining in adjacent regions being subtracted, and the average immunofluorescence intensity was calculated across all serial sections from every mouse used. The primary antibodies used were: anti-p62 (guinea pig, 1:400, MBL) and anti-CaMKIIα(mouse monoclonal [6G9], 1:500, Stressmarq).

Human transcriptome analysis

Human postmortem brain samples were obtained after consent from next of kin during autopsies conducted at the Allegheny County Medical Examiner's Office (Pittsburg, PA, USA) using procedures approved by the Institutional Review Board and Committee for Oversight of Research Involving the Dead at the University of Pittsburgh, as published in our previous report (44). A total of 51 MDD and 50 control subjects were included in the 8 studies in this report. Samples from the dorsolateral prefrontal cortex (dlPFC), subgenual anterior cingulate cortex (sgACC) or rostral amygdala enriched in lateral, basolateral and basomedial nuclei had been previously collected and processed on Affymetrix HG-U133 Plus 2 or Illumina HT12 gene arrays. Four studies were performed in the sgACC, 2 studies in the amygdala and 2 in the dlPFC. Half of the studies had been performed in female subjects in each brain region. Details on subjects, areas investigated and other parameters are described (44).

Statistical analysis

All data were represented as mean ± standard error of the mean (SEM) and were analyzed by Kruskal−Wallis test followed by Dunn's multiple comparison test, unless otherwise noted.

Behavioral assay data were analyzed by one-way or two-way analysis of variance (ANOVA) followed by Bonferroni post-hoc test, using Prism statistics software (GraphPad). Statistical significance in figures: $*P < 0.05$, $**P < 0.01$, $***P < 0.001$

ACKNOWLEDGEMENTS

We thank Dr. Albert Wong for permission to use the startle chamber. This work was supported by grants from the National Institutes of Health (MH-093723 to E.S.), Campbell Family Mental Health Research Institute (to E.S.), and Department of Defense/Congressionally Directed Medical Research Program (W81XWH-11-1-0269 to T.T.).

CONFLICTS OF INTEREST

The authors declare no conflicts of interest.

AUTHOR CONTRIBUTIONS

T.T., A.S., and Y.H.-T. carried out experiments; H.M. generated CaMKII-p62 transgenic mice; H.O. provided analytical tools; L.F. analyzed human transcriptome data; T.T. and E.S. wrote and edited the paper.

REFERENCES

1. Knight MJ, Baune BT. Cognitive dysfunction in major depressive disorder. *Curr Opin Psychiatry* 31, 26–31 (2018).

2. Bast T, Pezze M, McGarrity S. Cognitive deficits caused by prefrontal cortical and hippocampal neural disinhibition. *Br J Pharmacol* 174, 3211–3225 (2017).

3. Negrón-Oyarzo I, Aboitiz F, Fuentealba P. Impaired functional connectivity in the prefrontal cortex: a mechanism for chronic stress-induced neuropsychiatric disorders. *Neural Plast* 2016, 7539065 (2016).

4. Drevets WC, Price JL, Furey ML. Brain structural and functional abnormalities in mood disorders: implications for neurocircuitry models of depression. *Brain Struct Funct* 213, 93–118 (2008).

5. Trivedi MH, Rush AJ, Wisniewski SR, Nierenberg AA, Warden D, Ritz L, Norquist G, Howland RH, Lebowitz B, McGrath PJ, Shores-Wilson K, Biggs MM, Balasubramani GK, Fava M; STAR*D Study Team. Evaluation of outcomes with citalopram for depression using measurement-based care in STAR*D: implications for clinical practice. *Am J Psychiatry* 163, 28–40 (2006).

6. Carhart-Harris RL, Nutt DJ. Serotonin and brain function: a tale of two receptors. *J Psychopharmacol* 31, 1091–1120 (2017).

7. Blier P, El Mansari M. Serotonin and beyond: therapeutics for major depression. *Philos Trans R Soc Lond B Biol Sci* 368, 20120536 (2013).

8. Zanos P, Thompson SM, Duman RS, Zarate CA Jr, Gould TD. Convergent mechanisms underlying rapid antidepressant action. *CNS Drugs* 32, 197–227 (2018).

9. Tripp A, Oh H, Guilloux JP, Martinowich K, Lewis DA, Sibille E. Brain-derived neurotrophic factor signaling and subgenual anterior cingulate cortex dysfunction in major depressive disorder. *Am J Psychiatry* 169, 1194–1202 (2012).

10. Guilloux JP, Douillard-Guilloux G, Kota R, Wang X, Gardier AM, Martinowich K, Tseng GC, Lewis DA, Sibille E. Molecular evidence for BDNF- and GABA-related dysfunctions in the amygdala of female subjects with major depression. *Mol Psychiatry* 17, 1130–1142 (2012).

11. Islam F, Mulsant BH, Voineskos AN, Rajji TK. Brain-derived neurotrophic factor expression in individuals with schizophrenia and healthy aging: testing the accelerated aging hypothesis of schizophrenia. *Curr Psychiatry Rep* 19, 36 (2017).

12. Pillai A, Kale A, Joshi S, Naphade N, Raju MS, Nasrallah H, Mahadik SP. Decreased

BDNF levels in CSF of drug-naive first-episode psychotic subjects: correlation with plasma BDNF and psychopathology. *Int J Neuropsychopharmacol* 13, 535–539 (2010).

13. Favalli G, Li J, Belmonte-de-Abreu P, Wong AH, Daskalakis ZJ. The role of BDNF in the pathophysiology and treatment of schizophrenia. *J Psychiatr Res* 46, 1–11 (2012). Review. PMID: 22030467

14. Oh H, Lewis DA, Sibille E. The role of BDNF in age-dependent changes of excitatory and inhibitory synaptic markers in the human prefrontal cortex. *Neuropsychopharmacology* 41, 3080–3091 (2016).

15. Calabrese F, Guidotti G, Racagni G, Riva MA. Reduced neuroplasticity in aged rats: a role for the neurotrophin brain-derived neurotrophic factor. *Neurobiol Aging* 34, 2768–2776 (2013).

16. Lu B, Nagappan G, Lu Y. BDNF and synaptic plasticity, cognitive function, and dysfunction. *Handb Exp Pharmacol* 220, 223–250 (2014).

17. Dincheva I, Glatt CE, Lee FS. Impact of the BDNF Val66Met polymorphism on cognition: implications for behavioral genetics. *Neuroscientist* 18, 439–451 (2012). Review. PMID: 22367929

18. Dincheva I, Lynch NB, Lee FS. The role of BDNF in the development of fear learning. *Depress Anxiety* 33, 907–916 (2016). Review. PMID: 27699937

19. Chao MV. Neurotrophins and their receptors: a convergence point for many signalling pathways. *Nat Rev Neurosci* 4, 299–309 (2003).

20. Chao MV, Rajagopal R, Lee FS. Neurotrophin signalling in health and disease. *Clin Sci (Lond)* 110, 167–173 (2006).

21. Sánchez-Sánchez J, Arévalo JC. A review on ubiquitination of neurotrophin receptors: facts and perspectives. *Int J Mol Sci* 18, pii: E630 (2017).

22. Lippai M, Lőw P. The role of the selective adaptor p62 and ubiquitin-like proteins in autophagy. *Biomed Res Int* 2014, 832704 (2014). Review. PMID: 25013806

23. Northoff G, Sibille E. Cortical GABA neurons and self-focus in depression: a model linking cellular, biochemical and neural network findings. *Mol Psychiatry* 19, 959 (2014).

24. Maciag D, Hughes J, O'Dwyer G, Pride Y, Stockmeier CA, Sanacora G, Rajkowska G. Reduced density of calbindin immunoreactive GABAergic neurons in the occipital cortex in major depression: relevance to neuroimaging studies. *Biol Psychiatry* 67, 465–470 (2010).

25. Fee C, Banasr M, Sibille E. Somatostatin-positive gamma-aminobutyric acid interneuron

deficits in depression: cortical microcircuit and therapeutic perspectives. *Biol Psychiatry* 82, 549–559 (2017).

26. Hoftman GD, Datta D, Lewis DA. Layer 3 Excitatory and inhibitory circuitry in the prefrontal cortex: developmental trajectories and alterations in schizophrenia. *Biol Psychiatry* 81, 862–873 (2017). Review. PMID: 27455897

27. Caballero A, Tseng KY. GABAergic function as a limiting factor for prefrontal maturation during adolescence. *Trends Neurosci* 39, 441–448 (2016).

28. Porges EC, Woods AJ, Edden RA, Puts NA, Harris AD, Chen H, Garcia AM, Seider TR, Lamb DG, Williamson JB, Cohen RA. Frontal gamma-aminobutyric acid concentrations are associated with cognitive performance in older adults. *Biol Psychiatry Cogn Neurosci Neuroimaging* 2, 38–44 (2017). PMID: 28217759

29. Engin E, Zarnowska ED, Sigal M, Keist R, Zeller A, Pearce RA, Rudolph U. Alpha5-containing GABAA receptors in dentate gyrus enable cognitive flexibility. *FASEB J* 27, 661.7–661.7 (2013).

30. Kellendonk C, Simpson EH, Kandel ER. Modeling cognitive endophenotypes of schizophrenia in mice. *Trends Neurosci* 32, 347–358 (2009). PMID: 19409625

31. Parnaudeau S, O'Neill PK, Bolkan SS, Ward RD, Abbas AI, Roth BL, Balsam PD, Gordon JA, Kellendonk C. Inhibition of mediodorsal thalamus disrupts thalamofrontal connectivity and cognition. *Neuron* 77, 1151–1162 (2013). PMID: 23522049

32. Kononenko NL, Claßen GA, Kuijpers M, Puchkov D, Maritzen T, Tempes A, Malik AR, Skalecka A, Bera S, Jaworski J, Haucke V. Retrograde transport of TrkB-containing autophagosomes via the adaptor AP-2 mediates neuronal complexity and prevents neurodegeneration. *Nat Commun* 8, 14819 (2017).

33. Mizushima N, Komatsu M. Autophagy: renovation of cells and tissues. *Cell* 147, 728–741 (2011).

34. Mizushima N, Yamamoto A, Matsui M, Yoshimori T, Ohsumi Y. In vivo analysis of autophagy in response to nutrient starvation using transgenic mice expressing a fluorescent autophagosome marker. *Mol Biol Cell* 15, 1101–1111 (2004).

35. Mizushima N, Yoshimori T, Levine B. Methods in mammalian autophagy research. *Cell* 140, 313–326 (2010).

36. Pankiv S, Clausen TH, Lamark T, Brech A, Bruun JA, Outzen H, Øvervatn A, Bjørkøy G, Johansen T. p62/SQSTM1 binds directly to Atg8/LC3 to facilitate degradation of ubiquitinated protein aggregates by autophagy. *J Biol Chem* 282, 24131–24145 (2007). PMID: 17580304

37. Wang H, Bedford FK, Brandon NJ, Moss SJ, Olsen RW. GABA(A)-receptor-associated protein links GABA(A) receptors and the cytoskeleton. *Nature* 397, 69–72 (1999).

38. Boudreau AC, Milovanovic M, Conrad KL, Nelson C, Ferrario CR, Wolf ME. A protein crosslinking assay for measuring cell surface expression of glutamate receptor subunits in the rodent brain after in vivo treatments. *Curr Protoc Neurosci* CHAPTER: Unit–5.3019. (2012).

39. Manning EE, van den Buuse M. BDNF deficiency and young-adult methamphetamine induce sex-specific effects on prepulse inhibition regulation. *Front Cell Neurosci* 7, 92 (2013).

40. Swerdlow NR, Braff DL, Geyer MA. Sensorimotor gating of the startle reflex: what we said 25 years ago, what has happened since then, and what comes next. *J Psychopharmacol* 30, 1072–1081 (2016). Review.

41. Parikh V, Naughton SX, Yegla B, Guzman DM. Impact of partial dopamine depletion on cognitive flexibility in BDNF heterozygous mice. *Psychopharmacol (Berl)* 233, 1361–1375 (2016). PMID: 26861892

42. Bissonette GB, Martins GJ, Franz TM, Harper ES, Schoenbaum G, Powell EM. Double dissociation of the effects of medial and orbital prefrontal cortical lesions on attentional and affective shifts in mice. *J Neurosci* 28, 11124–11130 (2008).

43. Cho KK, Hoch R, Lee AT, Patel T, Rubenstein JL, Sohal VS. Gamma rhythms link prefrontal interneuron dysfunction with cognitive inflexibility in *Dlx*5/6$^{+/-}$ mice. *Neuron* 85, 1332–1343 (2015).

44. Ding Y, Chang LC, Wang X, Guilloux JP, Parrish J, Oh H, French BJ, Lewis DA, Tseng GC, Sibille E. Molecular and genetic characterization of depression: overlap with other psychiatric disorders and aging. *Mol Neuropsychiatry* 1, 1–12 (2015).

45. Huang DW, Sherman BT, Lempicki RA. Systematic and integrative analysis of large gene lists using DAVID Bioinformatics Resources. *Nat Protoc* 4, 44–57 (2009).

46. Huang DW, Sherman BT, Lempicki RA. Bioinformatics enrichment tools: paths toward the comprehensive functional analysis of large gene lists. *Nucleic Acids Res* 37, 1–13 (2009).

47. Laudes T, Meis S, Munsch T, Lessmann V. Impaired transmission at corticothalamic excitatory inputs and intrathalamic GABAergic synapses in the ventrobasal thalamus of heterozygous BDNF knockout mice. *Neuroscience* 222, 215–227 (2012).

48. Hauser J, Rudolph U, Keist R, Möhler H, Feldon J, Yee BK. Hippocampal alpha5 subunit-containing GABAA receptors modulate the expression of prepulse inhibition. *Mol Psychiatry* 10, 201–207 (2005).

49. Vilchez D, Saez I, Dillin A. The role of protein clearance mechanisms in organismal ageing and age-related diseases. *Nat Commun* 5:5659 (2014).

50. Salminen A, Kaarniranta K, Haapasalo A, Hiltunen M, Soininen H, Alafuzoff I. Emerging role of p62/sequestosome-1 in the pathogenesis of Alzheimer's disease. *Prog Neurobiol* 96, 87–95 (2012).

51. Ferrer I, Martinez A, Blanco R, Dalfó E, Carmona M. Neuropathology of sporadic Parkinson disease before the appearance of parkinsonism: preclinical Parkinson disease. *J Neural Transm (Vienna)* 118, 821–839 (2011).

52. Nagy A, Gertsenstein M, Vintersten K, Behringer R. Manipulating the mouse embryo. A Laboratory Manual. 3rd Edition. Cold Spring Harbor Laboratory Press (2003).

53. Takahashi N, Sakurai T, Bozdagi-Gunal O, Dorr NP, Moy J, Krug L, Gama-Sosa M, Elder GA, Koch RJ, Walker RH, Hof PR, Davis KL, Buxbaum JD. Increased expression of receptor phosphotyrosine phosphatase-β/ζ is associated with molecular, cellular, behavioral and cognitive schizophrenia phenotypes. *Transl Psychiatry* 1, e8 (2011).

FIGURE LEGENDS

Figure 1. BDNF regulates autophagy in cortical neurons

(A) Primary cortical neurons prepared from GFP-LC3 mice were treated with BDNF (100 ng/ml) or vehicle for 30 min, and the fluorescence intensities of GFP+ autophagosomes and their size were scored from > 50 GFP+ puncta per condition. Scale bar, 20 μm. * $p < 0.05$ (Kruskal-Wallis test)

(B) Autophagy flux assay: primary cortical neurons were treated with BDNF (100 ng/ml) for the indicated times in the presence or absence of lysosomal protease inhibitor (bafilomycin A1 [BafA1], 5 ng/ml) and the cell lysates were analyzed by Western blot using LC3 antibody. * $p < 0.05$, ** $p < 0.01$ (Kruskal-Wallis test)

(C) Primary cortical neurons prepared from wild-type mice were transfected with GFP-LC3 and treated with BDNF (100 ng/ml) for 30 min. LysoTracker uptake was evaluated to measure acidity of the lysosome in culture. Scale bar, 20 μm. Dotted areas were magnified below. Arrows indicate GFP+ autophagosomes located in the neurite. * $p < 0.05$ (Kruskal-Wallis test)

Figure 2. Reduced BDNF expression leads to elevated p62 levels in cortical pyramidal

neurons

(A, B) The PFC (layer 2/3) of *Bdnf*$^{+/-}$ mice (n = 4) and their WT littermates (n = 4) (2 to 2.5 months of age) were immunostained with p62 and their fluorescence intensities in CaMKII+ neurons were scored and plotted in (B). Scale bar, 20 μm. * $p < 0.05$ (Kruskal-Wallis test)

(C) Quantitative PCR analysis of autophagy-related genes expressed in the PFC of WT (n = 3) and *Bdnf*$^{+/-}$ mice (n = 3) (2 months of age). * $p < 0.05$, ** $p < 0.01$ (Kruskal-Wallis test)

Fig. 3. Decreased surface presentation of α5GABA$_A$R and behavioral deficits in *Bdnf*$^{+/-}$ mice are rescued by reducing *p62* gene dosage

(A) Surface biotinylation of primary cortical neurons prepared from WT, *Bdnf*$^{+/-}$, or *Bdnf*$^{+/-}$;*p62*$^{+/-}$ mice, analyzed by Western blot using the indicated antibodies. Surface levels of expression were normalized by the total levels of expression for each genotype. The assays were performed in triplicate. * $p < 0.05$ (Kruskal-Wallis test)

(B) BS3 cross-linking assays using the PFC extracts from WT, *Bdnf*$^{+/-}$, or *Bdnf*$^{+/-}$;*p62*$^{+/-}$ mice. Levels of non-crosslinked α5GABAAR (~50 kDa) were normalized by levels of αTubulin at each time point. Differences in the levels of non-crosslinked α5GABAAR at a given time point

vs. those of the control sample (No Xlink: no cross-linker added) represent the amount of surface α5GABAAR that underwent mobility shift toward a higher molecular weight range due to covalent crosslinking with anonymous cell surface proteins. * $p < 0.05$ (Kruskal-Wallis test)

(C) The amplitude of startle response and the percentage of PPI were evaluated for WT ($n = 10$), *Bdnf*$^{+/-}$ ($n = 10$), and *Bdnf*$^{+/-}$;*p62*$^{+/-}$ mice ($n = 10$). No significant difference in startle response ($F_{2,27} = 0.378$, $P = 0.9243$, one-way ANOVA). Statistical significance for %PPI; $F_{2,27} = 9.775$, $P < 0.001$ (two-way ANOVA with repeated measures); * $p < 0.05$ (Bonferroni post-hoc test).

(D) Schematic diagram of the rule shift assay: Mice were habituated to food, feeding apparatus, different odor cues (O1, O2, etc.; e.g., coriander vs. garlic powder) and texture cues (TA, TB, etc.; e.g., fine vs. coarse digging media) prior to testing, and then food-deprived a day before the assays. Mice were initially trained in a sequence of trials to associate a food reward with a specific stimulus (*i.e.*, either an odor or a digging medium; a stimulus associated with food reward is shown in red). A varying combination of stimulus and food reward was presented to mice per trial. Eight consecutive correct responses to the food reward were considered reaching criterion (*i.e.*, successful establishment of association between the stimulus and the food reward), and the number of trials to reach criterion were scored for each mouse tested, before

and after rule shifting (*e.g.*, from an odor cue to a different texture cue to predict reward).

(E) Numbers of trials to criterion were scored for WT (n = 6), *Bdnf*$^{+/-}$ (n = 6), and *Bdnf*$^{+/-}$;*p62*$^{+/-}$ mice (n = 6) during the initial association phase, as well as the rule shift phase of the assays. No significant difference during the initial association phase ($F_{2,15}$ = 1.25, P = 0.934). Statistical significance during the rule shift phase: $F_{2,15}$ = 9.93, P < 0.001 (one-way ANOVA); ** p < 0.01 (Bonferroni post-hoc test).

Fig. 4. Elevated p62 expression is sufficient to cause downregulation of surface α5GABA$_A$R expression and the behavioral deficits

(A) Generation of CaMKII-p62-transgenic mouse lines. Among 3 lines established, 2 lines (#1, #3) showed ~60% higher levels of p62 protein expression in the PFC when compared with WT, whereas the line #2 showed no apparent increase in p62 expression. * p < 0.05 (Kruskal-Wallis test)

(B) BS3 cross-linking assays using the PFC extracts from WT, p62-Tg#1 and Tg#2 mice. Levels of non-crosslinked α5GABAAR (~50 kDa) were normalized by levels of αTubulin at each time point. * p < 0.05 (Kruskal-Wallis test)

(C) The amplitude of startle response and the percentage of PPI were evaluated for WT (n = 10), p62-Tg#1 (n = 10), p62-Tg#2 (n = 10), and p62-Tg#3 mice (n = 10). No significant difference in startle response ($F_{3,36}$ = 0.726, P = 0.7121, one-way ANOVA). Statistical significance for %PPI; $F_{3,36}$ = 12.474, P < 0.001 (two-way ANOVA with repeated measures); * p < 0.05 (Bonferroni post-hoc test).

(D) Numbers of trials to criterion were scored for WT (n = 7) and p62-Tg#1 mice (n = 7) during the initial association phase, as well as the rule shift phase of the assays. No significant difference during the initial association phase ($F_{1,12}$ = 0.843, P = 0.857). Statistical significance during the rule shift phase: $F_{1,12}$ = 10.67, P < 0.001 (one-way ANOVA); ** p < 0.01 (Bonferroni post-hoc test).

Fig. 5. Gene expression profiling with human postmortem brains suggest altered autophagy machinery in MDD brains

(A) Expression levels of the autophagy-enhancing genes (98 genes, **Supplementary Table 1** and **2** combined) vs. the autophagy-attenuating genes (34 genes, **Supplementary Table 3**) in the corticolimbic area of the MDD brain cohorts were compared with those of the control

cohorts. Overall expression levels of the autophagy-attenuating genes in MDD, as represented by the area under the curve (AUC = 0.68) were significantly different from those of the autophagy-enhancing genes, as represented by the AUC (= 0.39) (P = 0.0077).

(B) The autophagy-attenuating genes in MDD tend to cluster toward the direction of upregulation, whereas the autophagy-enhancing genes in MDD tend to cluster toward the direction of downregulation. Levels of gene expression of *Somatostatin* (*SST*) and *BDNF* are significantly downregulated in the corticolimbic area of the MDD brains, as represented by the AUC value of 0.079 and 0.022, respectively.

Fig. 6. Two modes of mechanisms underlying GABA dysfunction following reduced BDNF signaling

Attenuated BDNF expression or signaling in the cortical pyramidal neurons, due to chronic stress or other neuropsychiatric insults, leads to GABA dysfunction through transcriptional suppression of GABA synapse genes in the neighboring inhibitory neurons (paracrine mode) (Ref. 14) and also via reduced surface presentation of α5-GABAAR in the pyramidal neurons (autocrine mode) (this study), together contributing to cognitive and other behavioral deficits

relevant to neuropsychiatric disorders, including MDD.

Figure 1

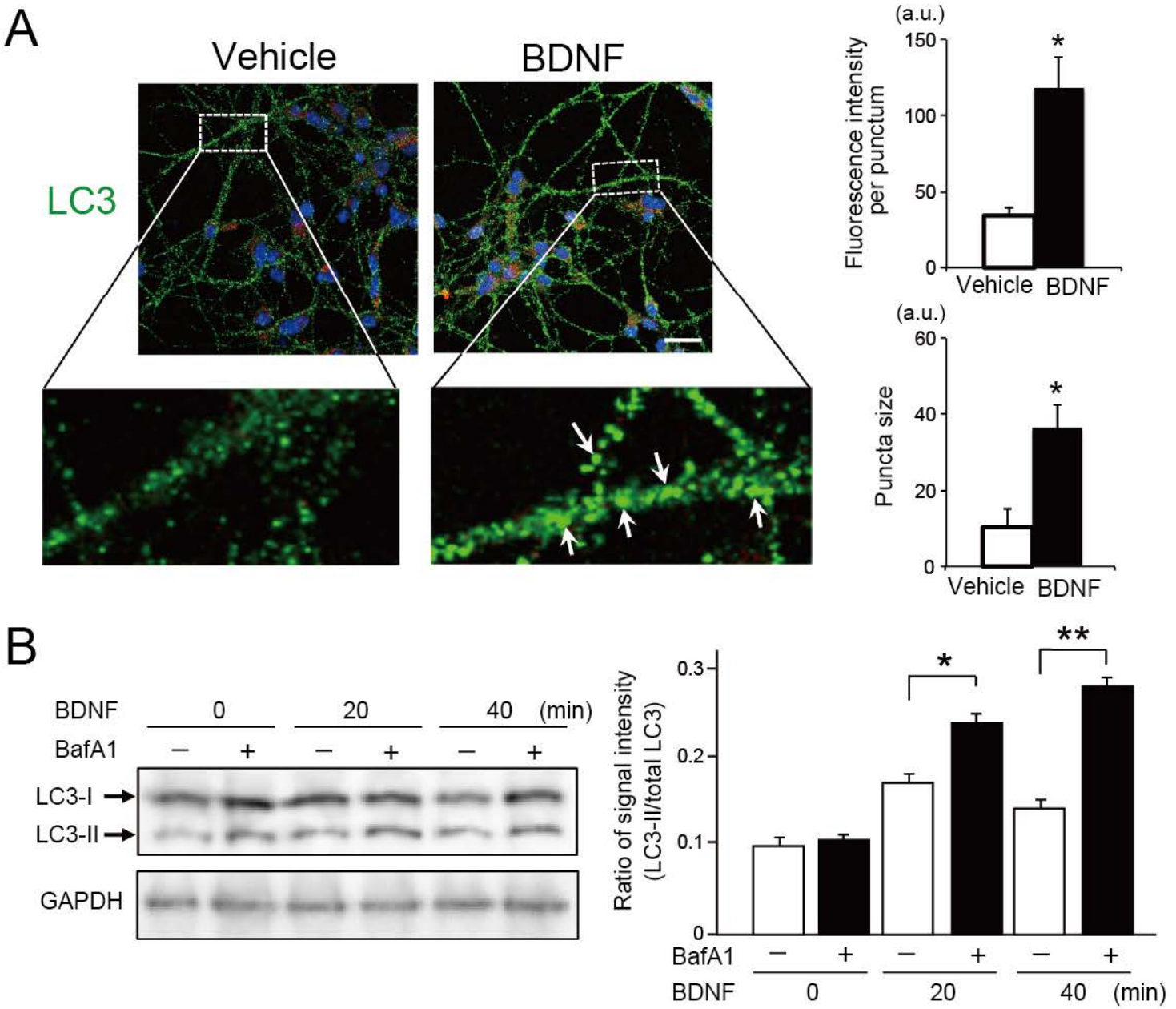
A
Vehicle
BDNF
LC3
(a.u.)
Fluorescence intensity per punctum
150
100
50
0
*
Vehicle
BDNF
(a.u.)
Puncta size
60
40
20
0
*
Vehicle
BDNF
B
BDNF
0
20
40
(min)
BafA1
−
+
−
+
−
+
LC3-I
LC3-II
GAPDH
Ratio of signal intensity (LC3-II/total LC3)
0.3
0.2
0.1
0
*
**
BafA1
−
+
−
+
−
+
BDNF
0
20
40
(min)

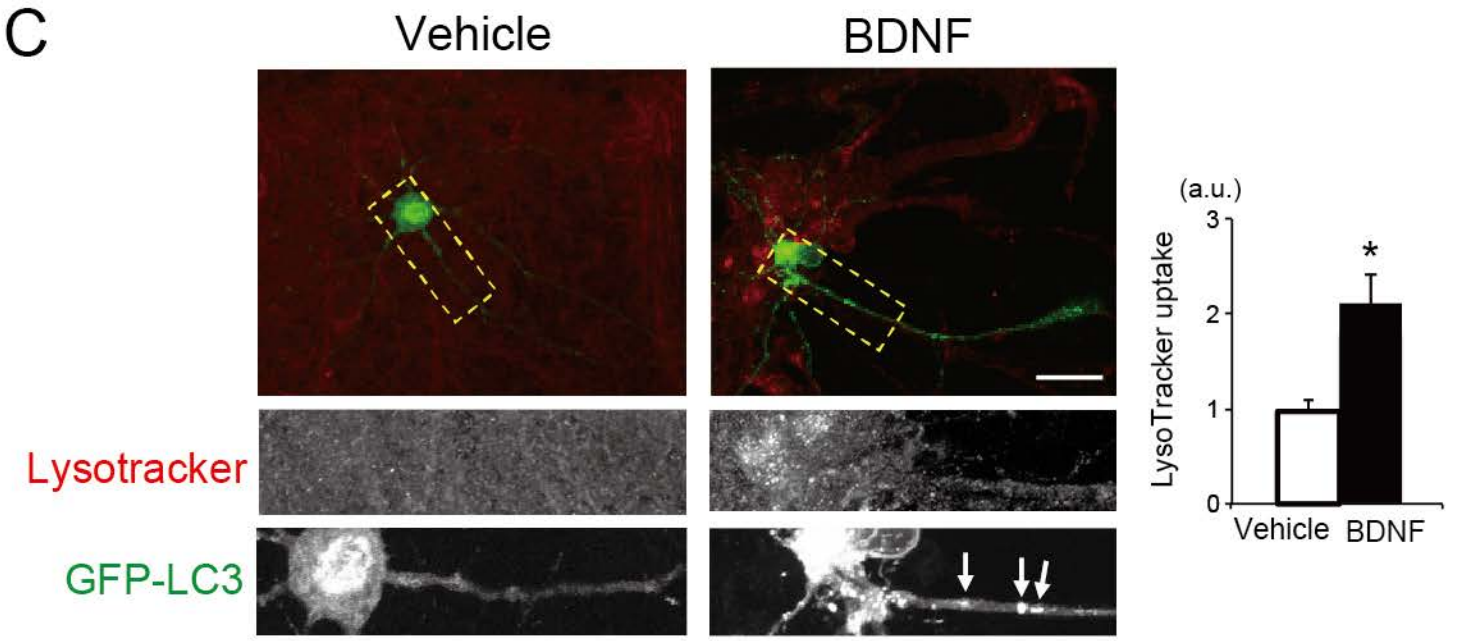
C
Vehicle
BDNF
Lysotracker
GFP-LC3
(a.u.)
LysoTracker uptake
3
2
1
0
*
Vehicle
BDNF

Figure 2

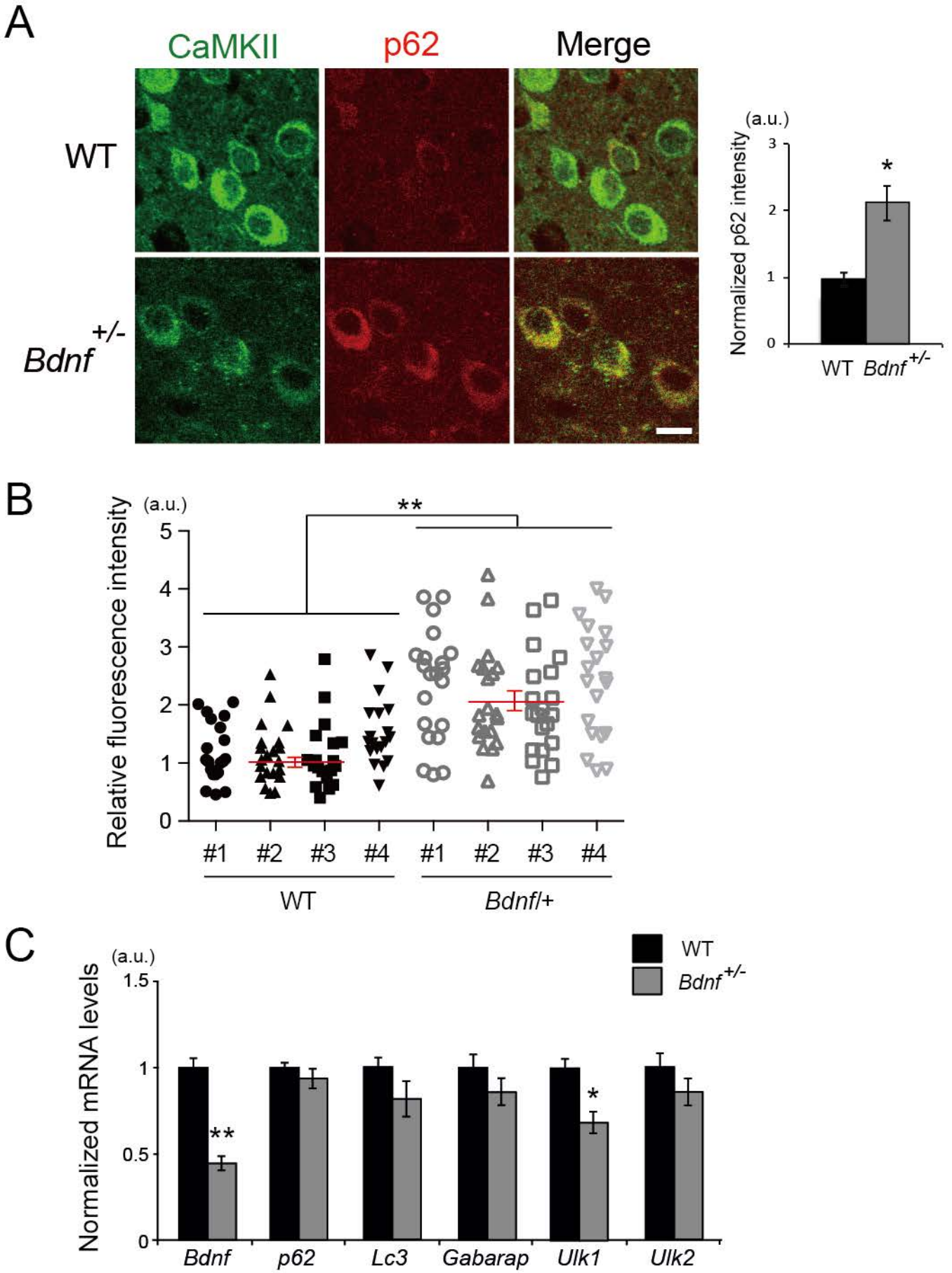
A
CaMKII
p62
Merge
WT
Bdnf+/-
(a.u.)
Normalized p62 intensity
3
2
1
0
*
WT
Bdnf+/-
B
(a.u.)
Relative fluorescence intensity
5
4
3
2
1
0
**
#1
#2
#3
#4
#1
#2
#3
#4
WT
Bdnf/+
C
(a.u.)
Normalized mRNA levels
1.5
1
0.5
0
WT
Bdnf+/-
**
*
Bdnf
p62
Lc3
Gabarap
Ulk1
Ulk2

Figure 3

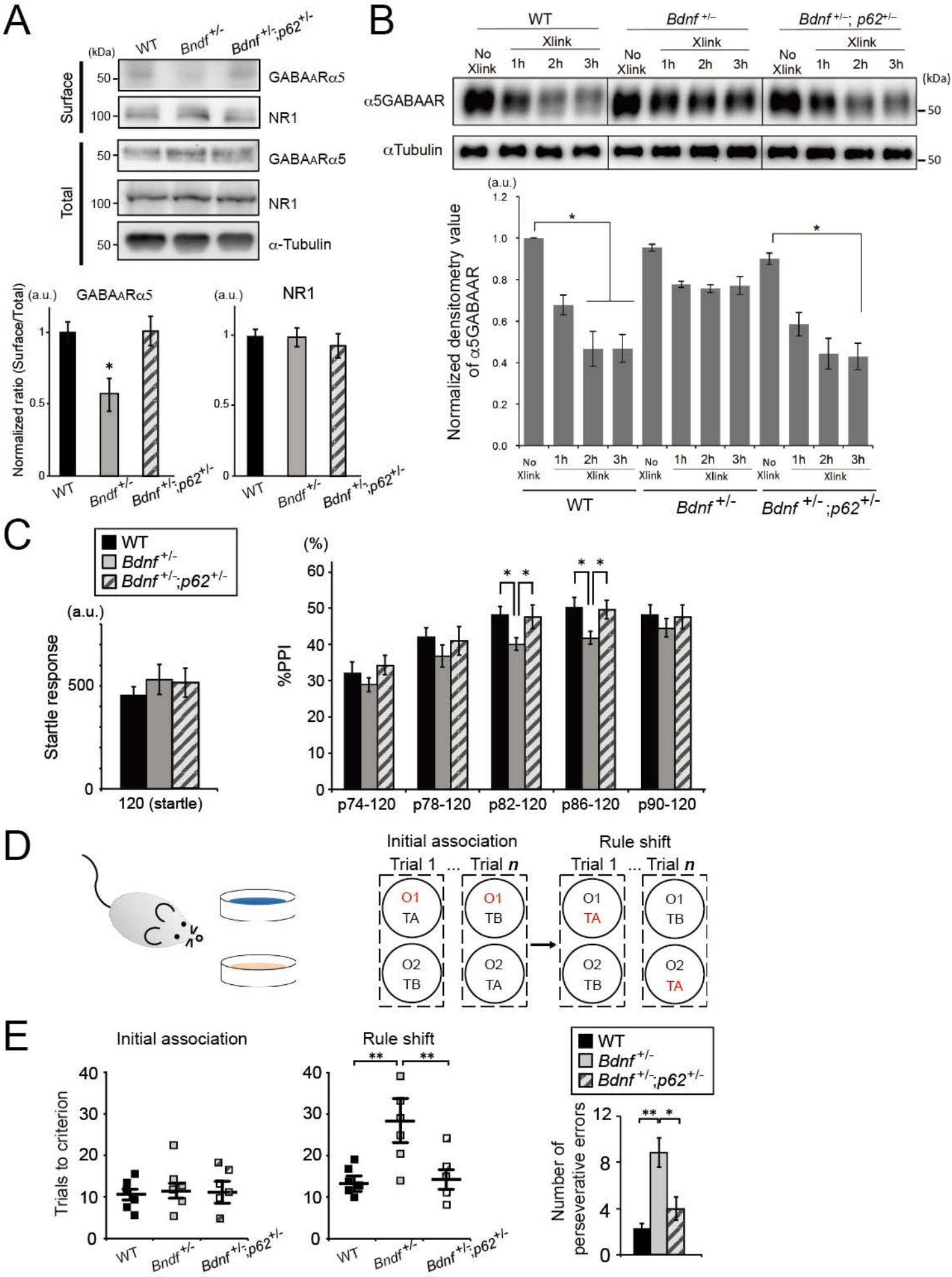
A
(kDa)
WT
Bndf+/-
Bndf+/-;p62+/-
Surface
Total
50
100
GABAARα5
NR1
α-Tubulin
Normalized ratio (Surface/Total)
(a.u.)
GABAARα5
NR1
B
WT
Bdnf +/–
Bdnf +/–; p62+/–
Xlink
No Xlink
1h
2h
3h
α5GABAAR
αTubulin
(kDa)
Normalized densitometry value of α5GABAAR
C
WT
Bdnf+/-
Bdnf+/-;p62+/-
Startle response
120 (startle)
%PPI
p74-120
p78-120
p82-120
p86-120
p90-120
D
Initial association
Rule shift
Trial 1
... Trial n
O1
TA
TB
O2
E
Initial association
Rule shift
Trials to criterion
Number of perseverative errors

Figure 4

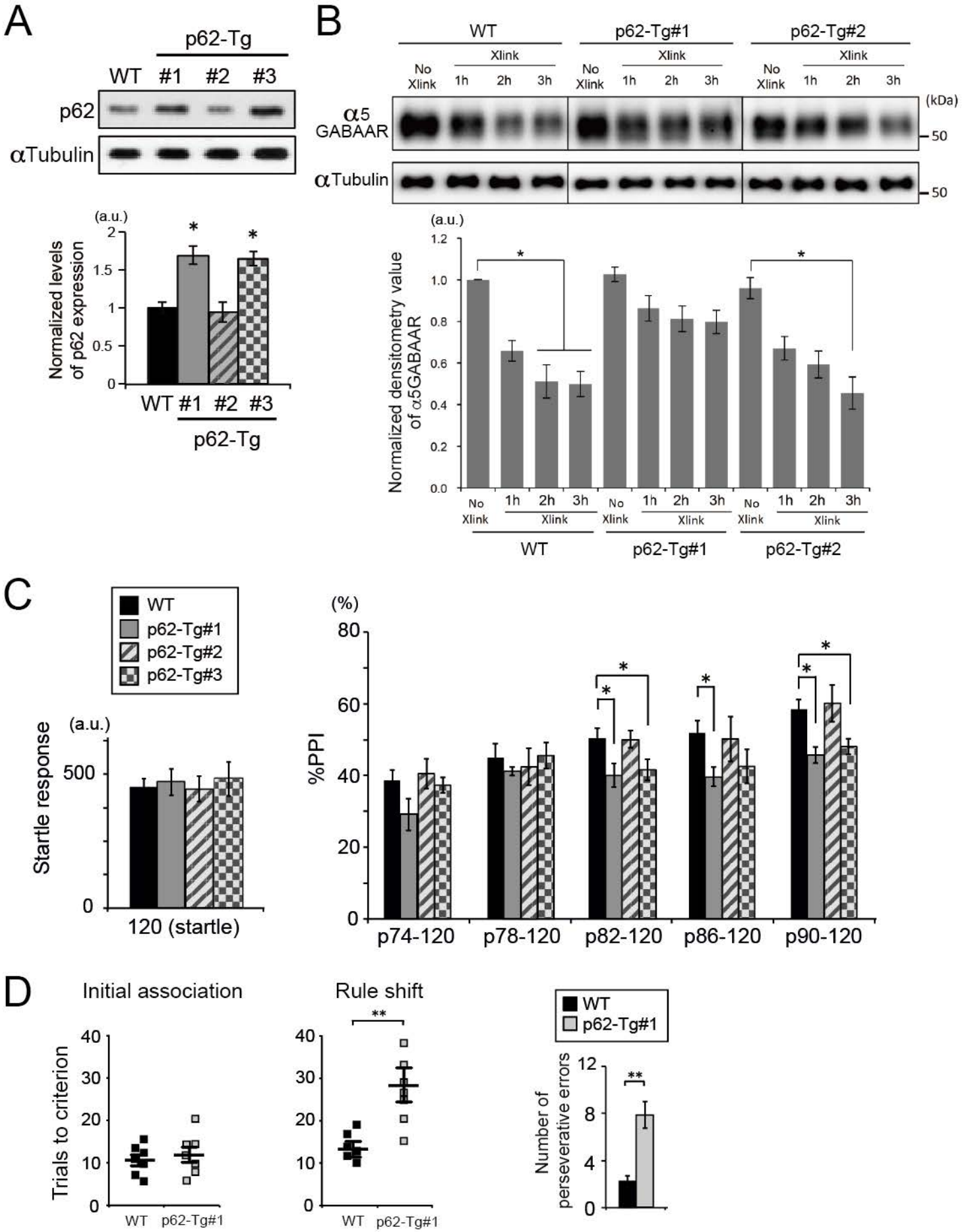
A
p62-Tg
WT #1 #2 #3
p62
αTubulin
Normalized levels of p62 expression
(a.u.)
WT #1 #2 #3
p62-Tg
B
WT
p62-Tg#1
p62-Tg#2
Xlink
No Xlink 1h 2h 3h
α5 GABAAR
αTubulin
(kDa)
50
Normalized densitometry value of α5GABAAR
(a.u.)
C
WT
p62-Tg#1
p62-Tg#2
p62-Tg#3
Startle response
(a.u.)
120 (startle)
%PPI
(%)
p74-120
p78-120
p82-120
p86-120
p90-120
D
Initial association
Rule shift
Trials to criterion
WT
p62-Tg#1
Number of perseverative errors

Figure 5

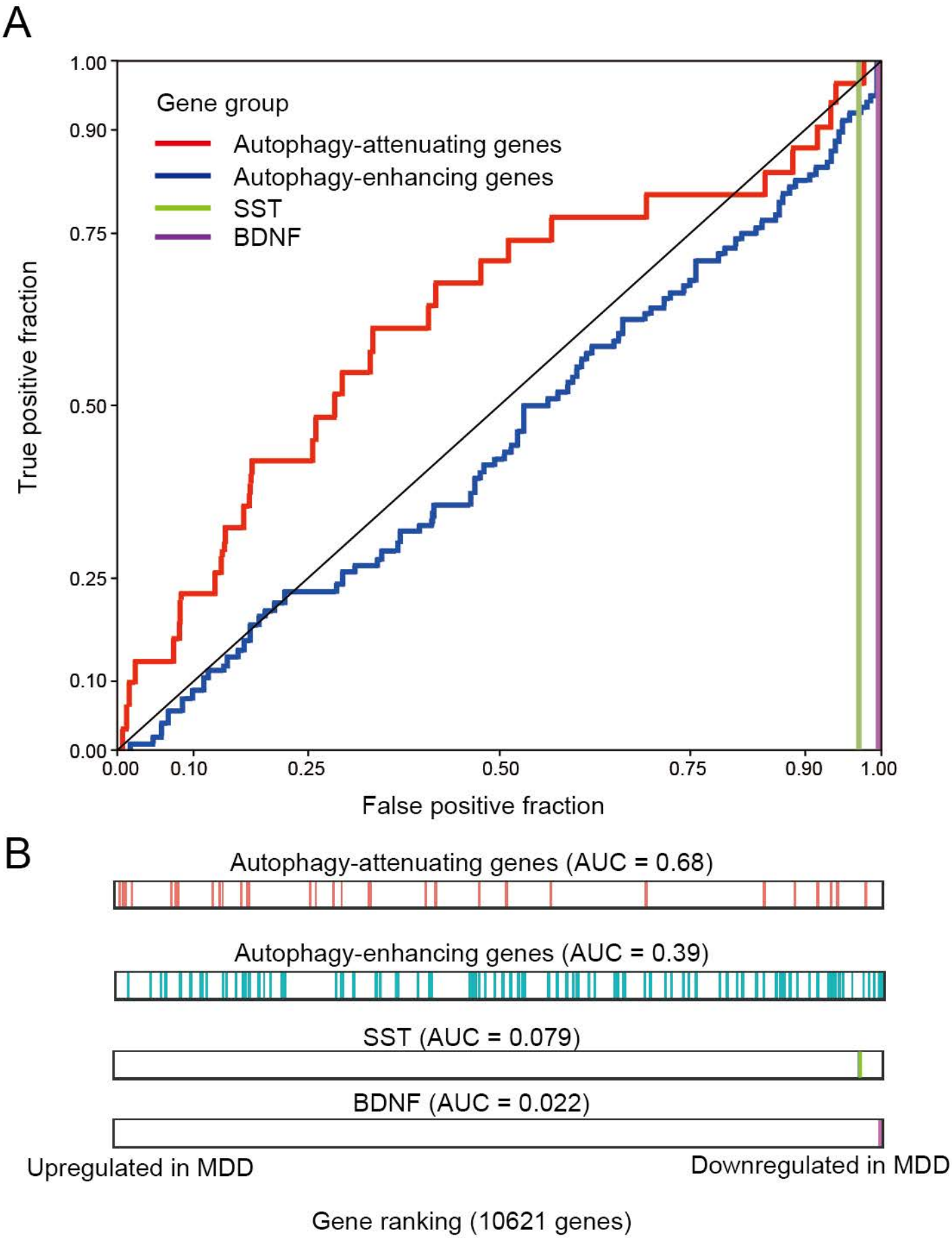
A
Gene group
Autophagy-attenuating genes
Autophagy-enhancing genes
SST
BDNF
True positive fraction
False positive fraction
1.00
0.90
0.75
0.50
0.25
0.10
0.00
0.00
0.10
0.25
0.50
0.75
0.90
1.00
B
Autophagy-attenuating genes (AUC = 0.68)
Autophagy-enhancing genes (AUC = 0.39)
SST (AUC = 0.079)
BDNF (AUC = 0.022)
Upregulated in MDD
Downregulated in MDD
Gene ranking (10621 genes)

Figure 6

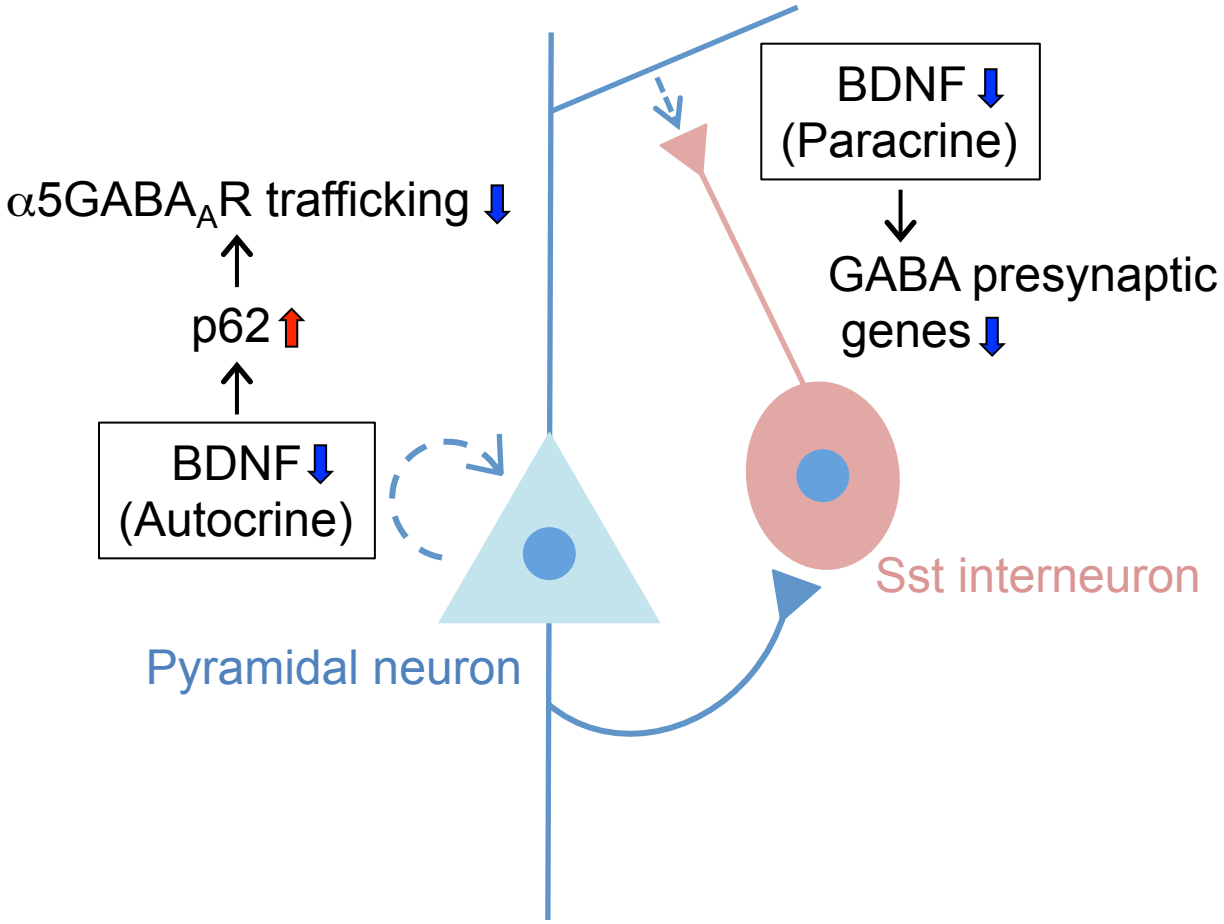
BDNF ⬇
(Paracrine)
GABA presynaptic genes ⬇
α5GABA$_A$R trafficking ⬇
p62 ⬆
BDNF ⬇
(Autocrine)
Sst interneuron
Pyramidal neuron

Supplementary Table 1

Supplementary Table 1. Customized list of the autophagy-enhancing genes

gene_symbol	p_value_aw	medianEffect
EIF2AK4	0.034984747	1.162669369
TRIM8	0.117535166	0.818133331
SMCR8	0.152032012	1.27782292
DAPK1	0.155987666	0.770628523
ATPIF1	0.173100273	1.553535083
FYCO1	0.22174155	0.700398633
AMBRA1	0.222481311	0.855662055
SUPT5H	0.2542512	0.887141728
SESN2	0.296281612	0.289254212
LRRK2	0.310434987	0.724924336
TICAM1	0.366607476	0.621448164
SH3BP4	0.382627436	0.474681386
FOXO1	0.417930421	0.719989416
PIP4K2B	0.441107052	0.897350304
MAPK3	0.457994539	0.776615843
SIRT1	0.489636852	0.84425061
TP53INP2	0.510219565	0.603880019
MID2	0.531684964	1.165562608
PRKAA2	0.570616138	0.071009746
KIAA1324	0.720906977	1.158383241
PIP4K2C	0.740623576	0.098748746
CLEC16A	0.769017701	0.366000548
KDR	0.829098108	0.950940013
TPCN1	0.838233782	0.105844955
RALB	0.879007721	0.559178164
RAB3GAP1	0.87990999	0.227513656
HDAC6	0.88163092	0.698590534
WAC	0.932930515	0.284368044
MFN2	0.960825911	0.012070394
SPTLC2	0.9638599	0.138458922
OPTN	0.934316825	−0.158996104
MTDH	0.926198663	−0.158968805
CALCOCO2	0.920138405	−0.693186218
HTRA2	0.912784201	−0.097381324
SCOC	0.875743904	−0.130406807
TBK1	0.851887581	−0.067948212
PAFAH1B2	0.815563412	−0.308292491
HIF1A	0.814421523	−0.266228513

gene_symbol	p_value_aw	medianEffect
UVRAG	0.807666792	−0.352264888
VPS13C	0.805675172	−0.420452464
BECN1	0.801819885	−0.411825619
DHRSX	0.744477639	−0.199340534
FBXO7	0.722127389	−0.037960469
TFEB	0.700580266	−0.018485743
CAMKK2	0.684909236	−1.566969409
RAB12	0.675408813	−0.942742606
PARK7	0.670962621	−0.143228124
TRIM22	0.645755579	−0.257948582
BNIP3L	0.63394445	−0.458369868
RIPK2	0.584106581	−0.575034615
STK11	0.564148668	−1.371998267
TSC1	0.56266651	−0.381984843
BNIP3	0.497204595	−0.535210457
PLK2	0.463951888	−0.532009937
PIK3CB	0.448217588	−1.412430676
FLCN	0.412448545	−0.97800392
TRIM13	0.397255626	−0.012605542
PLEKHF1	0.394280388	−0.76786282
EPM2A	0.322975238	−0.639018648
TSC2	0.300476697	−0.370809509
PRKAA1	0.286510875	−1.267519244
PIM2	0.240186706	−0.754203311
SH3GLB1	0.203863007	−1.221496301
SPTLC1	0.194087845	−1.544333353
LARP1	0.180830995	−0.861198852
MAP3K7	0.099798795	−0.823531047
LRSAM1	0.096247717	−1.217880954
C9orf72	0.092959608	−1.288356398
GSK3B	0.077148197	−1.615224996
TMEM59	0.070357029	−0.926792913
CDC37	0.051240185	−1.009629071
PINK1	0.029979192	−1.11375343
IKBKG	0.01017456	−1.031605376
PRKD1	0.003644101	−1.210506542
BAD	0.00279823	−1.347739423
DCN	0.00053366	−1.634289599

Supplementary Table 2. Customized list of the autophagy maturation genes

gene_symbol	p_value_aw	medianEffect
SNX14	0.147074663	0.675692116
VPS33A	0.672570756	0.904040607
SNAP29	0.74007777	0.125522767
VCP	0.834424819	0.401512237
VPS16	0.83737859	0.519108401
LIX1	0.932354581	−0.273249391
CALCOCO2	0.920138405	−0.693186218
UVRAG	0.807666792	−0.352264888
LAMP2	0.702094436	−0.388714965
GABARAPL2	0.575407589	−0.584347403
CLN3	0.50934347	−0.764568165
STX17	0.423380567	−0.528784357
GABARAP	0.398240467	−0.204459714
VAMP8	0.343637134	−0.585788979
TSG101	0.259045476	−0.850928386
SNAPIN	0.212957443	−0.864722301
TBC1D25	0.202719141	−0.681825632
MCOLN1	0.166698522	−0.248693735
MAP1LC3A	0.087320874	−1.023047875
PHF23	0.079421335	−0.608212865
UBQLN1	0.018410413	−1.477666864
LIX1L	0.001097072	−1.922553403

Supplementary Table 3. Customized list of the autophagy-attenuating genes

gene_symbol	p_value_aw	medianEffect
EIF4G1	0.015020149	1.437745811
KIF25	0.023130496	1.190166014
DAP	0.030276057	0.770542156
AKT1	0.055029187	1.326819928
SIRT2	0.197292157	1.515489055
UBQLN4	0.213909236	0.844394059
GOLGA2	0.219871575	1.017417495
WDR6	0.340445438	0.364700969
CHMP4A	0.35986216	1.067377846
MT3	0.37116458	0.599926824
MTM1	0.439070332	0.047310997
TBC1D14	0.454628943	0.909881069
CTSA	0.461122681	0.417650653
CHMP4B	0.648297053	0.468667816
BCL2	0.663554844	0.959336518
PIK3CA	0.715826288	0.757406388
RASIP1	0.739175407	0.225829356
TSPO	0.812726674	0.137934588
SCFD1	0.817457961	0.658080788
QSOX1	0.955435835	0.180495981
NPC1	0.97898503	0.774296622
TLK2	0.910991997	−0.218861268
LARS	0.841193673	−0.339605394
NRBP2	0.735582054	−0.206637359
RNF5	0.504352321	−0.048494504
HERC1	0.235670276	−1.184952443
RNF41	0.167279729	−1.393432626
LZTS1	0.120550042	−1.481081734
RRAGA	0.090564919	−0.559871294
PHF23	0.079421335	−0.608212865
POLDIP2	0.022472272	−1.070552502